

Trajectory tracking control of kites with system delay

J. H. Baayen*

December 27, 2012

Abstract

A previously published algorithm for trajectory tracking control of tethered wings, i.e. kites, is updated in light of recent experimental evidence. The algorithm is, furthermore, analyzed in the framework of delay differential equations. It is shown how the presence of system delay influences the stability of the control system, and a methodology is derived for gain selection using the Lambert W function. The validity of the methodology is demonstrated with simulation results. The analysis sheds light on previously poorly understood stability problems.

1 Introduction

During the past two decades researchers have taken an increasing interest in the industrial applications of tethered wings, i.e., kites. Two well-known applications include the towing of ships [14] and wind- to electrical power conversion [13, 3]. An integral part of both technologies is autonomous kite flight along a prescribed trajectory, relative to the earth surface attachment point. Various control principles have been proposed, see, e.g. [8, 5, 2, 7, 16, 11]. This paper discusses the influence of system delays on trajectory tracking performance. The issue of system delays has been raised before in [8], where a wireless link is part of the control loop, and in [5], where actuator delay is identified. Up to now, however, no rigorous analysis of the effect of delay on system performance has been carried out.

A small kite such as the one shown in Figure 1 is highly sensitive to control inputs, and hence to system delay. The ability to fly such small wings smoothly with minimal control expenditure therefore hinges on an accurate treatment of their fast dynamics. We use the theory of delay differential equations to incorporate system delay into the stability analysis of a kite trajectory tracking control algorithm.

We base our analysis on the controller previously laid out in [2]. Since its initial publication, the algorithm has been applied in practice (Figure 1), and in the process, has undergone several revisions. In the next section, we commence by summarizing our algorithm in its most recent form. We then discuss the stability of an elementary linear differential equation with delay. Noting that

*Baayen & Heinz GmbH, Sekr. ER2-1, Hardenbergstraße 36a, 10623 Berlin, Germany, jorn.baayen@baayen-heinz.com.



Figure 1: A 5 m² de-power kite on a 40 m line in automated flight. Composite photo taken near Schöneiche, Germany, on February 22, 2012.

our inner loop controller shapes the system into a delayed linear system of the same type, we proceed to identify its region of stability and, in a certain sense, optimal control gain. In the final section we demonstrate the applicability of the result in simulation.

2 Trajectory tracking control

In [2] we showed how the turning, or path, angle of the kite trajectory can be used to formulate a cascaded single-input single-output control problem. In this section we briefly recapitulate this result, and present several modifications which have turned out to improve performance in practice.

First of all, the presence of the kite's tether constrains its movement to a sphere centered on the tether's earth surface attachment point. In our analysis, the radius of this sphere turns out to be irrelevant, and therefore we restrict our attention to the unit sphere centered on the origin.

Restricted to the unit sphere, we can speak of geodesic, or great-circle, distances

$$\text{dist}(\mathbf{p}, \mathbf{q}) := \arccos(\mathbf{p} \cdot \mathbf{q}),$$

as well as of tangent planes. After defining a basis in the tangent bundle, we can measure the angle between any tangent vector and the primary basis vector. For vectors tangent to a curve, this angle is known as the turning angle [10] – in this paper denoted as θ (Figure 2).

In [2] we defined the steering control input, u , as the length difference of the kite steering lines. We showed how this control input u can be used to control the direction of flight, represented by the turning angle θ . Secondly, we used spherical geometry to derive an outer loop control law that selects a target turning angle, θ_t , such as to guarantee convergence to the target trajectory.

A commonly prescribed target trajectory is the crosswind, lying figure of eight (Figure 1). This trajectory has a bounded winding number, thereby avoiding problems with lines winding around themselves and each other.

We now proceed to summarize the inner and outer loop control laws.

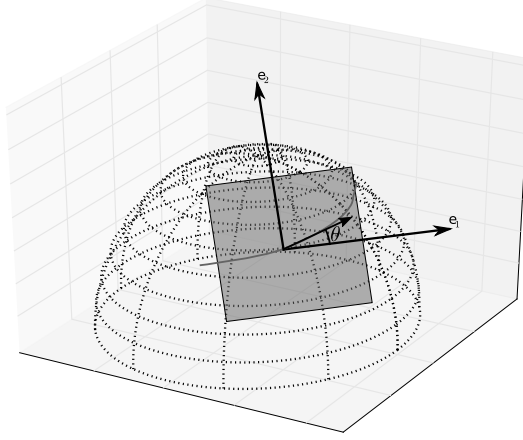


Figure 2: The notion of turning, or path, angle θ .

2.1 Inner loop

In [5] it is, based on experimental evidence, claimed that

$$\dot{\theta} = KV_a u, \quad (1)$$

with proportionality factor K , airspeed V_a , and steering control input u .¹ The linear structure of Equation 1 obsoletes the incremental feedback-linearizing approach previously taken by us in [2], and thereby simplifies matters significantly.

However, the airspeed V_a is also a function of the turning angle, and hence also a function of the steering control input u . Implicit in Equation 1 is the assumption that the influence of the control input u acts on the turning rate $\dot{\theta}$ more quickly than it acts on the airspeed V_a . We return to this time-scale separation in Section 4.

Proposition 2.1. *Consider the system given by Equation 1. The control law*

$$u := \frac{1}{KV_a}(\dot{\theta}_t + P(\theta_t - \theta)),$$

with gain $P \in \mathbb{R}^+$, renders the Lyapunov function

$$V := \frac{1}{2}(\theta_t - \theta)^2$$

decreasing along the flow.

Proof. Expand dV/dt . □

Future work on the inner loop may focus on the incorporation of actuator dynamics using, e.g., backstepping [12].

¹In [5], the turning angle θ is called the “orientation angle”, denoted ψ .

2.2 Outer loop

As the kite moves along its trajectory, γ , the desired target point $\gamma_t(s)$ must slide along on the target trajectory, γ_t . To this end, we continuously locate the target point closest to the present kite location, i.e.,

$$s(t) := \operatorname{argmin}_s \operatorname{dist}(\gamma(t), \gamma_t(s)). \quad (2)$$

This optimization problem is not convex. But, since we desire to track a smoothly changing target location, we welcome local minima. A simple gradient descent [9] performs well for this purpose. When initialized with the solution from the previous timestep, the method converges within a handful of iterations. Unlike the method we originally proposed in [2], this method does not suffer from drift of the target location.

In the following we will, for brevity, identify γ_t with the composition $\gamma_t \circ s$. Once a target point has been determined using Equation 2, a target turning angle needs to be selected. To this end, let \mathbf{T}_t denote the unit vector tangent to the target trajectory. Let $\mathbf{T} := \mathbf{R}^T \mathbf{T}_t$, where the operator \mathbf{R} rotates γ to γ_t along their connecting geodesic, so that \mathbf{T} is an element of the tangent plane at γ . Let $\mathbf{t} := \gamma \times \mathbf{T}$, so that the vectors \mathbf{T} and \mathbf{t} form a basis of the tangent plane at γ . Finally, denote

$$\gamma_t^\perp := \gamma_t - (\gamma_t \cdot \gamma)\gamma.$$

By selecting the target flight direction as an appropriately weighted sum of the “direction along the target” \mathbf{T} , and the “direction towards the target” \mathbf{t} , we obtain tracking convergence:

Proposition 2.2 (Baayen, 2012 [2]). *The turning angle θ_t determined by*

$$\cos \theta_t \mathbf{e}_1 + \sin \theta_t \mathbf{e}_2 = \operatorname{normalize}(\mathbf{T} + L(\mathbf{t} \cdot \gamma_t^\perp)\mathbf{t}), \quad (3)$$

with gain $L \in \mathbb{R}^+$, renders the geodesic distance

$$W := \operatorname{dist}(\gamma, \gamma_t)$$

*decreasing along the flow.*²

3 A delay differential equation

We now introduce an elementary linear delay differential equation, which in Section 4 will prove to be a valuable tool for analyzing the stability of our kite control system in face of delay.

Let

$$\frac{dy}{dt}(t) = ky(t - \tau), \quad (4)$$

with $k \in \mathbb{R}$, a linear differential equation with delay τ . With the change of variables $s = t/\tau$ and $x(s) = y(\tau s)$, we obtain the equation in its canonical form

$$\frac{dx}{ds}(s) = ax(s - 1), \quad (5)$$

²In the original paper, the required normalization is missing. For practical applications this does not matter, as the trigonometric computation of θ_t is only a function of the direction of the vector, not of its norm. Thanks to Dipl.-Ing. Claudius Jehle for pointing this out.

with $a = \tau k$.

Unlike its relative without delay, Equation 5 admits oscillatory solutions. For example, when $a = -\pi/2$, it is readily verified that

$$x = \sin\left(\frac{\pi}{2}s\right)$$

provides such a solution. Hence it is not the case that a negative coefficient in Equations 4 or 5 guarantees convergence to the zero-solution. We must therefore consider these equations in more detail.

It turns out that the solution space of Equation 5 is infinite-dimensional [6]. This circumstance is hardly surprising, considering that we need to specify initial conditions over an interval. Any solution can be written as

$$x = \sum_n \lambda_n e^{\sigma_n s},$$

with the coefficients λ_n determined by the initial conditions, and σ_n the roots of the characteristic equation

$$\sigma - ae^{-\sigma} = 0.$$

The roots of the characteristic equation, σ_n , are given by the set-valued Lambert W function:

$$\{\sigma_n\} = W(a).$$

The real part of the first several branches of the Lambert W function is shown in Figure 3.

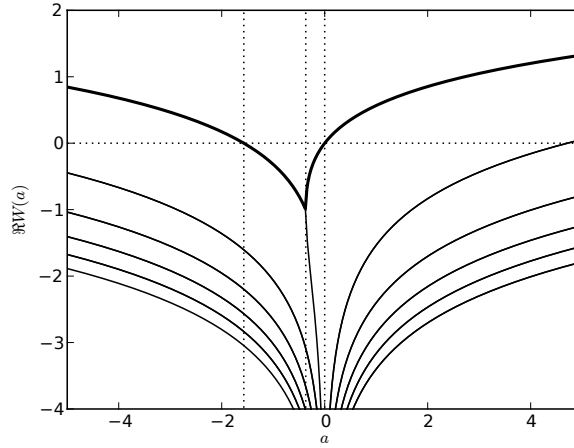


Figure 3: Real part of the Lambert W function, branches -5 to 5 , with the principal branch highlighted in bold.

We proceed to analyze the stability of Equation 5. Let W_k denote the k th branch of the Lambert W function. Figure 3 hints at the following Lemma:

Lemma 3.1 (Shinozaki and Mori, 2006 [15]). *The real part of the principal branch of the Lambert W function is no less than that of any other branch, i.e.,*

$$\max\{\Re(W_k(z)) | k = 0, \pm 1, \dots, \pm\infty\} = \Re(W_0(z)).$$

Lemma 3.2. *The zero-solution of Equation 5 is globally stable if*

$$-\pi/2 \leq a \leq 0.$$

Proof. The proof follows directly from Lemma 3.1, Figure 3, and the observations that $W(-\pi/2) \ni i\pi/2$ and $W(0) \ni 0$. \square

Lemma 3.3. *The quickest worst-case convergence to the zero-solution of Equation 5 is guaranteed if*

$$a = -\frac{1}{e},$$

irrespective of the initial conditions.

Proof. The proof follows directly from Lemma 3.1, Figure 3, and from the fact that W is not differentiable at $-1/e$ [4]. \square

4 Trajectory tracking control with delay

In the present section we modify the results from Section 2 to incorporate a system delay τ .

First of all, we recall the time-scale separation of the turning rate $\dot{\theta}$ and the airspeed V_a implicit in Equation 1. The turning angle θ specifies the direction of flight. Considering that the direction of flight acts on the position indirectly through integration, we can expect another time-scale separation between the flight direction and the position dynamics.

In the following we show how this structure can be exploited to analyze stability in face of system delays.

4.1 Inner loop

The outer loop control law given by Equation 3 is a function of position only. By time-scale separation, this implies that the resulting target turning angle θ_t varies slowly compared to the time constant of the inner loop. In the present discussion of the inner loop we therefore assume that $d\theta_t/dt = 0$.

Exploiting this assumption and following Section 3, we obtain the following stability criterion:

Proposition 4.1. *Consider the turning rate law with delay τ :*

$$\dot{\theta}(t) = KV_a(t)u(t - \tau), \tag{6}$$

cf. Equation 1. Assume that $d\theta_t/dt = 0$, and let $P \in (0, \frac{\pi}{2\tau})$. Then the control law

$$u := \frac{1}{KV_a}P(\theta_t - \theta) \tag{7}$$

renders $\theta \rightarrow \theta_t$. Furthermore, this convergence is optimal in the sense of Lemma 3.3 when

$$P = \frac{1}{e\tau}.$$

Proof. Substituting Equation 7 into the system given by Equation 6, and using our assumption that $d\theta_t/dt = 0$, we obtain the controlled system

$$\frac{d}{dt}(\theta_t - \theta)(t) = -P(\theta_t - \theta)(t - \tau). \quad (8)$$

From Lemma 3.2, we obtain that the controlled system given by Equation 8 is stable if $-\pi/2 \leq -P\tau \leq 0$. \square

This quantifies what we already know from practice, namely, that the inner loop control gain P cannot be arbitrarily large. Proposition 4.1 aids us in selecting a gain appropriate for the specific system implementation at hand.

4.2 Outer loop

The outer loop treats the target direction θ_t as a virtual control input, capable of being commanded pseudo-instantaneously. This assumption is motivated by the time-scale separation. The target turning angle θ_t will be commanded to the inner loop without delay within the same control software cycle.

Furthermore, we assume the system delay τ to be insignificant compared to the time scale of the position dynamics. As we will be able to verify with the simulation results from the next section, the system delay is typically a small fraction of the flight time of a figure of eight.³ Hence, we do not include delay in our analysis of the outer loop.

5 Simulation results

In [1] we show how one may simulate a kite system using potential flow computations and a discretized tether. Using an identical system setup, we now present several simulation results.

We start out by presenting a reference result without delay. Selecting an outer loop gain of $L = 5$ and an inner loop gain of $P = 10$, the target trajectory is tracked, for all practical purposes, perfectly. See Figures 4 and 5.

By introducing a delay of $\tau = 0.2$ s, the gain $P = 10$ lies outside of the range given by Proposition 4.1. As expected, this is reflected in the instability of the turning angle. See Figures 6 and 7.

Finally, by choosing $L = 5$ and the optimal inner loop gain $P = 1/(e\tau)$, we obtain the convergent trajectory and stable turning angle tracking of Figures 8 and 9. We note, however, that trajectory tracking performance suffers somewhat at the expense of stable turning angle tracking.

We conclude that Proposition 4.1 provides a useful tool for understanding, and eliminating, delay-induced instabilities observed in kite control systems.

6 Concluding remarks

In this paper we have presented, based on recent experimental evidence, a simplification of our previously published cascaded kite trajectory tracking control algorithm. Furthermore, we have shown how the Lambert W function can be

³In contrast, a kite can be made to spin rapidly about its tether.

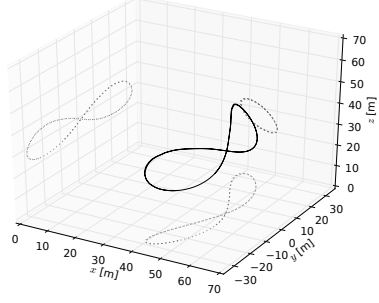


Figure 4: Trajectory with $\tau = 0$ s, $L = 5$, and $P = 10$.

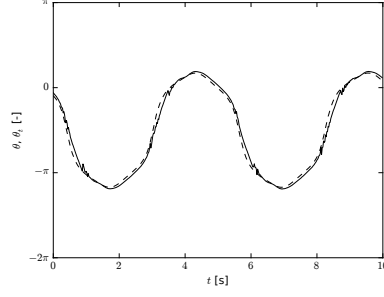


Figure 5: Turning angle (solid) with target (dashed), $\tau = 0$ s, $L = 5$, and $P = 10$.

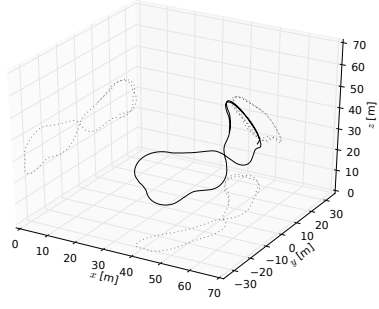


Figure 6: Trajectory with $\tau = 0.2$ s, $L = 5$, and $P = 10$.

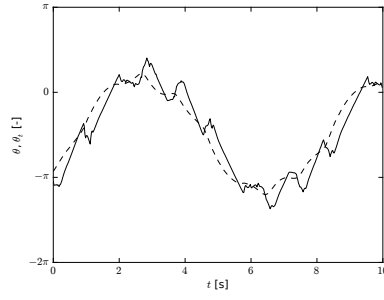


Figure 7: Turning angle (solid) with target (dashed), $\tau = 0.2$ s, $L = 5$, and $P = 10$.

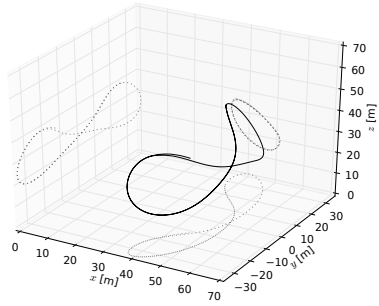


Figure 8: Trajectory with $\tau = 0.2$ s, $L = 5$, and $P = 1/(e\tau)$.

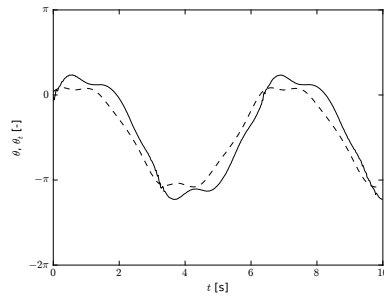


Figure 9: Turning angle (solid) with target (dashed), $\tau = 0.2$ s, $L = 5$, and $P = 1/(e\tau)$.

used to analyze the stability of kite trajectory tracking control systems with delay. We demonstrated how such an analysis leads to a methodology for gain selection in face of delay. Finally, we demonstrated the validity of our approach with simulation results.

Future research may focus on the influence of actuator dynamics on inner control loop performance, and similarly, on the influence of inner loop dynamics on the performance of the outer loop.

References

- [1] J. H. Baayen. Vortexje - an open-source panel method for co-simulation, 2012, arXiv:1210.6956.
- [2] J. H. Baayen and W. J. Ockels. Tracking control with adaption of kites. *IET Journal of Control Theory & Applications*, 6(2):182–191, 2012.
- [3] M. Canale, L. Fagiano, and M. Milanese. Power kites for wind energy generation. *IEEE Control Systems Magazine*, 27(6):25–38, 2007.
- [4] R. M. Corless, G. H. Gonnet, D. E. G. Hare, D. J. Jeffrey, and D. E. Knuth. On the LambertW function. *Advances in Computational Mathematics*, 5(1):329–359, 1996.
- [5] M. Erhard and H. Strauch. Control of towing kites for seagoing vessels. *Control Systems Technology, IEEE Transactions on*, PP(99):1, 2012.
- [6] T. Erneux. *Applied delay differential equations*. Springer, 1st edition, 2009.
- [7] L. Fagiano. *Control of Tethered Airfoils for High-Altitude Wind Energy Generation*. PhD thesis, Politecnico di Torino, Torino, 2009.
- [8] U. Fechner and R. Schmehl. Design of a distributed kite power control system. In *IEEE Multi-Conference on Systems and Control*, Dubrovnik, Croatia, 2012.
- [9] R. Fletcher. *Practical Methods of Optimization*. Wiley, 2nd edition, 2000.
- [10] A. Gray. *Modern Differential Geometry of Curves and Surfaces with Mathematica*. CRC-Press, 2nd edition, 1997.
- [11] A. Ilzhöfer, B. Houska, and M. M. Diehl. Nonlinear MPC of kites under varying wind conditions for a new class of large scale wind power generators. *International Journal of Robust and Nonlinear Control*, 17(17):1590–1599, 2007.
- [12] H. K. Khalil. *Nonlinear systems*. Prentice Hall, 3rd edition, 2001.
- [13] M. L. Loyd. Crosswind kite power. *Journal of Energy*, 4(3):106–111, 1980.
- [14] P. Naaijen, V. Koster, and R. P. Dallinga. On the power savings by an auxiliary kite propulsion system. *International shipbuilding progress*, 53(4):255–279, 2006.

- [15] H. Shinozaki and T. Mori. Robust stability analysis of linear time-delay systems by Lambert W function: some extreme point results. *Automatica*, 42(10):1791–1799, 2006.
- [16] P. Williams, B. Lansdorp, and W. J. Ockels. Flexible tethered kite with moveable attachment points, part I: Dynamics and control. In *AIAA Atmospheric Flight Mechanics Conference and Exhibit*, Hilton Head, South Carolina, 2007.